

**Antiferromagnetic Kondo lattice NpNi<sub>2</sub>Sn**M. Szlawska,<sup>1</sup> K. Gofryk,<sup>2,3</sup> J.-C. Griveau,<sup>2</sup> E. Colineau,<sup>2</sup> P. Gaczyński,<sup>2</sup> R. Jardin,<sup>2</sup> R. Caciuffo,<sup>2</sup> and D. Kaczorowski<sup>1</sup><sup>1</sup>*Institute of Low Temperature and Structure Research, Polish Academy of Sciences, P. O. Box 1410, 50-950 Wrocław, Poland*<sup>2</sup>*European Commission, Joint Research Centre, Institute for Transuranium Elements, Postfach 2340, 76125 Karlsruhe, Germany*<sup>3</sup>*Los Alamos National Laboratory, Los Alamos, New Mexico 87545, USA*

(Received 12 December 2011; revised manuscript received 7 March 2012; published 25 April 2012)

The compound NpNi<sub>2</sub>Sn has been studied by means of x-ray diffraction, heat capacity, magnetic and electrical transport measurements performed over a wide range of temperatures and applied magnetic fields. The results revealed Kondo-lattice behavior and antiferromagnetic ordering below the Néel temperature of 13 K. The compound has been characterized as a moderately enhanced heavy-fermion system, one of very few known amidst Np-based intermetallics.

DOI: [10.1103/PhysRevB.85.134443](https://doi.org/10.1103/PhysRevB.85.134443)

PACS number(s): 75.50.Ee, 71.27.+a, 75.30.Mb

**I. INTRODUCTION**

For a few recent decades, uranium-based intermetallics have continuously been a subject of intense research. They show a wide variety of properties due to strong electronic correlations, including the formation of heavy-fermion ground states, non-Fermi-liquid behavior, quantum criticality, and/or magnetically driven superconductivity.<sup>1-3</sup> Much less studied have been compounds based on transuranium elements although also for them, especially for Np- and Pu-bearing phases, nontrivial physical behavior can be expected. Recently, investigations of this type of materials have been boosted due to the discovery of unconventional superconductivity in PuCoGa<sub>5</sub>, PuRhGa<sub>5</sub>, and NpPd<sub>5</sub>Al<sub>2</sub>.<sup>4-6</sup>

The uranium-based ternary phases with composition UT<sub>2</sub>M, where T stands for a *d*-electron transition metal and M is a *p*-electron element, have attracted much attention because of diversity in their intriguing physical behavior, predominantly driven by hybridization between 5*f*-electronic states and conduction-band states.<sup>7-15</sup> The findings made for UT<sub>2</sub>M stimulate our on-going research on related compounds based on transuranium elements. Recently, we reported on two novel phases NpPd<sub>2</sub>Sn and PuPd<sub>2</sub>Sn, which have been characterized as antiferromagnetically ordered Kondo lattices.<sup>16,17</sup> In the present study we focus on a related stannide NpNi<sub>2</sub>Sn. Its U-based counterpart forms with a cubic Heusler-type crystal structure and undergoes a transition to an orthorhombic structure at 220 K.<sup>18,19</sup> Below the structural transition, UNi<sub>2</sub>Sn exhibits some features characteristic of Kondo-like behavior.<sup>20</sup> The main aim of our study was to establish the formation of NpNi<sub>2</sub>Sn and to reveal its low-temperature magnetic- and electrical-transport properties.

**II. EXPERIMENTAL DETAILS**

A polycrystalline sample of NpNi<sub>2</sub>Sn was prepared by arc-melting the constituent elements in a Zr-gettered argon atmosphere. The starting components were high-purity elements (Np 3N, Ni 5N, and Sn 5N). The quality of the so-obtained material was checked at room temperature by powder x-ray diffraction using a Bruker D8 diffractometer with Cu *K*α radiation. It has been found that the sample was a single phase with an orthorhombic symmetry and lattice parameters *a* = 9.6106(6) Å, *b* = 4.3576(3) Å, and *c* = 6.5921(5) Å. The

revealed space group *Pnma* suggests that NpNi<sub>2</sub>Sn is isostructural with the compounds AnPd<sub>2</sub>Sn, where An = Th, U, Np, or Pu<sup>7,16,17</sup> and with the low-temperature phase of UNi<sub>2</sub>Sn.<sup>18</sup>

Magnetic-susceptibility measurements were performed within the temperature range 2–300 K and in magnetic fields up to 7 T, using a Quantum Design MPMS-7 superconducting quantum interference device magnetometer. The heat capacity and the electrical resistivity were studied in the temperature interval 2–300 K and in magnetic fields up to 9 T, employing a Quantum Design PPMS-9 platform. The Hall-coefficient measurements were carried out between 2 and 300 K and in a magnetic field of 14 T, using a Quantum Design PPMS-14 platform. The thermoelectric power was measured from 6 to 300 K using a homemade setup with pure copper as a reference material. The <sup>237</sup>Np Mössbauer spectra were recorded using a sinusoidal drive motion of a <sup>241</sup>Am-metal source kept at 4.2 K. The temperature of the absorber containing 127 mg Np/cm<sup>2</sup> was varied from 4.2 K to 25 K. The velocity scale of the spectrometer was calibrated with reference to a NpAl<sub>2</sub> absorber (*B*<sub>hf</sub> = 330 T at 4.2 K). Because of the radioactivity and toxicity of neptunium, samples were encapsulated using STYCAST® 2850 FT for all the experiments to avoid contamination risk. The measured data were corrected by applying a standard correction due to the average encapsulation contribution.

**III. RESULTS AND DISCUSSION****A. Magnetic properties**

Figure 1 shows the temperature dependence of the inverse molar magnetic susceptibility of NpNi<sub>2</sub>Sn measured in an applied magnetic field of 7 T. In the paramagnetic region, above 150 K, the  $\chi(T)$  variation can be well described by the Curie-Weiss law  $\chi(T) = \frac{\mu_{\text{eff}}^2}{8(T-\theta_p)}$  with the effective magnetic moment  $\mu_{\text{eff}} = 3.0 \mu_B$  and the paramagnetic Curie temperature  $\theta_p = -198$  K. The  $\chi(T)$  curve can also be represented in the wider temperature range down to 15 K by the modified Curie-Weiss law in the form  $\chi = \chi_0 + \frac{\mu_{\text{eff}}^2}{8(T-\theta_p)}$  with fitting parameters  $\mu_{\text{eff}} = 2.3 \mu_B$ ,  $\theta_p = -100$  K, and  $\chi_0 = 7 \times 10^{-4}$  emu/mol. Since 5*f* electrons are thought not to be localized in light actinides, it seems that the latter gives more reliable parameters. The so-obtained value of the magnetic

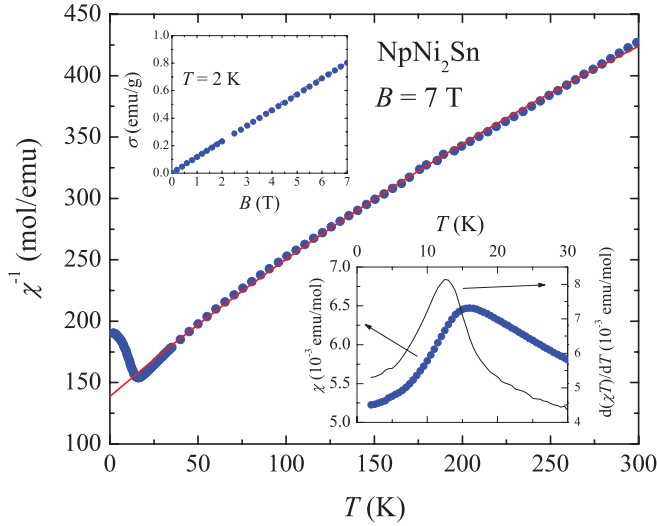


FIG. 1. (Color online) Temperature dependence of the reciprocal molar magnetic susceptibility of  $\text{NpNi}_2\text{Sn}$  measured in a field of 7 T. The solid line represents the fit of the modified Curie-Weiss law with the parameters given in the text. The upper inset presents the magnetic-field variation of the magnetization measured at a fixed temperature of 2 K. The lower inset displays the low-temperature magnetic-susceptibility data (left axis) and the temperature derivative of the  $\chi T$  product (right axis).

effective moment is smaller than that predicted for a free  $\text{Np}^{3+}$  ion within the intermediate coupling scheme ( $2.75 \mu_B$ ), and the value of  $\theta_p$  is large with a negative sign. Altogether, these two features may be attributed to strong hybridization of the  $5f$ -electronic states with the conduction-band states.

As displayed in the lower inset of Fig. 1, the magnetic susceptibility of  $\text{NpNi}_2\text{Sn}$  exhibits a pronounced maximum at 15 K that signals the onset of an antiferromagnetically ordered state. The Néel temperature, defined as an inflection point on the  $\chi T$  vs  $T$  variation<sup>21</sup> amounts to  $T_N = 13$  K (see the inset of Fig. 1). The magnetization measured at the terminal temperature of 2 K is proportional to the applied magnetic field strength (see the upper inset of Fig. 1). The absence of any metamagnetic-like anomaly up to the strongest field available (7 T) hints at significant magnetocrystalline anisotropy in the compound studied.

### B. Specific heat

The temperature dependence of the heat capacity of  $\text{NpNi}_2\text{Sn}$  up to 300 K is shown in the left inset of Fig. 2. Close to room temperature, the specific heat attains a value of about  $110 \text{ J mol}^{-1} \text{ K}^{-1}$ , which is somewhat larger than the Dulong-Petit limit, i.e.,  $C = 3nR = 99.77 \text{ J mol}^{-1} \text{ K}^{-1}$ , where  $n$  is the number of atoms per molecule and  $R$  is the gas constant. The antiferromagnetic phase transition at  $T_N = 13$  K manifests itself as a rather small anomaly in  $C(T)$ . In applied magnetic fields, the latter feature slightly shifts toward lower temperatures as expected for antiferromagnets (see the right inset of Fig. 2). As is obvious from Fig. 2, showing the  $C/T$  vs  $T^2$  variation, in the ordered region the heat capacity can be well approximated by the formula

$$C(T) = \gamma T + \beta T^3 + C_{\text{mag}}, \quad (1)$$

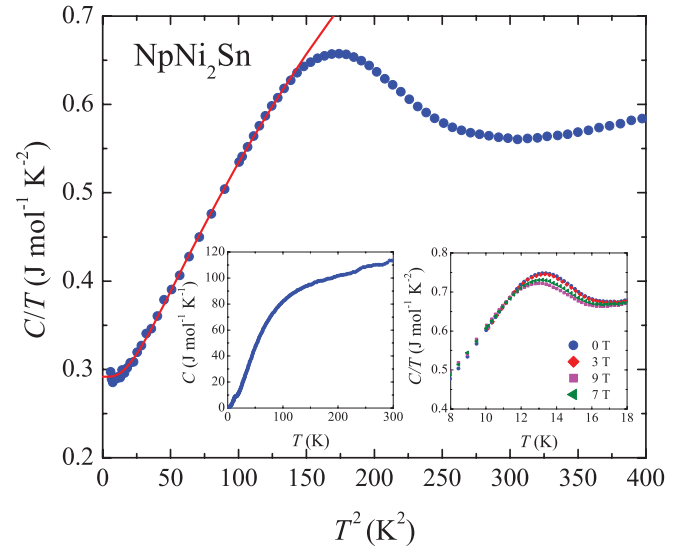


FIG. 2. (Color online) Heat capacity over temperature ratio of  $\text{NpNi}_2\text{Sn}$  as a function of squared temperature. The solid line represents the fit of Eq. (1) to the experimental data. The left inset shows the temperature dependence of the heat capacity up to 300 K. The right inset displays the specific heat over temperature ratio near the Néel temperature measured in various magnetic fields.

where the first term describes the electronic contribution to the heat capacity, the second term accounts for the phonon contribution, and the third term represents the magnetic contribution, expressed as<sup>22,23</sup>

$$C_{\text{mag}}(T) = c \Delta^{7/2} \sqrt{T} \exp(\Delta/T) \left[ 1 + \frac{39T}{20\Delta} + \frac{51}{32} \left( \frac{T}{\Delta} \right)^2 \right]. \quad (2)$$

The latter equation describes excitations of antiferromagnetic spin waves over a gap  $\Delta$  in the magnon spectrum and was derived assuming the dispersion relation  $\omega = \sqrt{\Delta^2 + Dk^2}$ , where  $D$  stands for the spin-wave stiffness. The coefficient  $c$  is related to  $D$  as  $c \propto D^{-3/2}$ . The least-squares fitting of these formulas to the experimental data of  $\text{NpNi}_2\text{Sn}$  yielded the following parameters:  $\gamma = 290 \text{ mJ mol}^{-1} \text{ K}^{-2}$ ,  $\beta = 4 \times 10^{-4} \text{ J mol}^{-1} \text{ K}^{-4}$ ,  $c = 8 \times 10^{-4} \text{ J mol}^{-1} \text{ K}^{-5}$ , and  $\Delta = 26$  K. The Sommerfeld coefficient  $\gamma$  is notably enhanced as expected for systems with strong electronic correlations. In turn, the magnitude of the spin-wave gap seems to be in good accord with the observed Néel temperature.

### C. Electrical resistivity

Figure 3 presents the electrical resistivity of  $\text{NpNi}_2\text{Sn}$ , measured as a function of temperature in zero applied magnetic field and in a field of 9 T. Generally, the resistivity is fairly large and changes only slightly in the temperature range studied. At 300 K, it amounts to about  $130 \mu\Omega \text{ cm}$ . With decreasing temperature down to about 25 K,  $\rho(T)$  exhibits a logarithmic increase, characteristic of Kondo systems. In this temperature range, the resistivity can be well approximated by the equation

$$\rho(T) = \rho_0 + \rho_0^\infty - c_K \ln T, \quad (3)$$

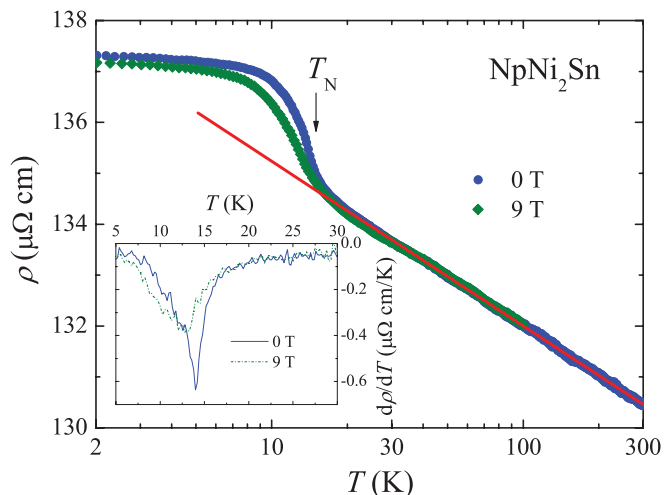


FIG. 3. (Color online) Temperature dependence of the electrical resistivity of NpNi<sub>2</sub>Sn, measured in a zero magnetic field and in a magnetic field of 9 T. The solid line denotes the logarithmic dependence in the paramagnetic state. The inset presents the temperature derivative of the resistivity at 0 and 9 T.

where the first and second terms account for the scattering of conduction electrons on lattice defects and disordered magnetic moments, respectively, whereas the third term describes the scattering on independent Kondo impurities. The least-squares fit of the above formula to the experimental data yielded  $\rho_0 + \rho_0^\infty = 138 \mu\Omega \text{ cm}$  and  $c_K = 1.4 \mu\Omega \text{ cm}$ .

The onset of the magnetic state at  $T_N = 13 \text{ K}$  manifests itself as an inflection point on the  $\rho(T)$  variation, better seen in the temperature derivative of the resistivity  $d\rho/dT(T)$  as a sharp Suezaki-Mori-type minimum<sup>24</sup> (see the inset of Fig. 3). Upon applying a magnetic field, this anomaly shifts to lower temperatures—in line with the corresponding heat-capacity data. In the antiferromagnetic region, the transverse magnetoresistance, defined as  $\Delta\rho/\rho = [\rho(B) - \rho(0)]/\rho(0)$ , is negative and rather small. Deeply in the ordered state, the absolute value of  $\Delta\rho/\rho$  is on the order of 0.1% only yet somewhat increases with increasing temperature toward  $T_N$ .

#### D. Hall effect

The temperature dependence of the Hall coefficient of NpNi<sub>2</sub>Sn is displayed in Fig. 4. At room temperature,  $R_H$  is positive and on the order of  $1 \times 10^{-10} \text{ m}^3/\text{C}$ . With decreasing temperature,  $R_H$  continuously increases and reaches a distinct maximum at the Néel temperature  $T_N = 13 \text{ K}$ . The overall behavior of  $R_H(T)$  is fairly similar to that of  $\chi(T)$ .

According to the theory by Fert and Levy,<sup>25</sup> the  $R_H(T)$  dependence of a dense Kondo system can be expressed by the equation

$$R_H(T) = R_0 + \gamma_1 \chi^*(T) \rho_{\text{mag}}(T), \quad (4)$$

where the first term  $R_0$  is the ordinary Hall coefficient due to the Lorentz force and skew scattering by residual defects whereas the second term represents the anomalous part that arises from magnetic skew scattering. In the above formula,  $\chi^*(T) = \chi(T)/C$  is the reduced magnetic susceptibility ( $C$  is the Curie constant) while  $\rho_{\text{mag}}$  is the magnetic contribution

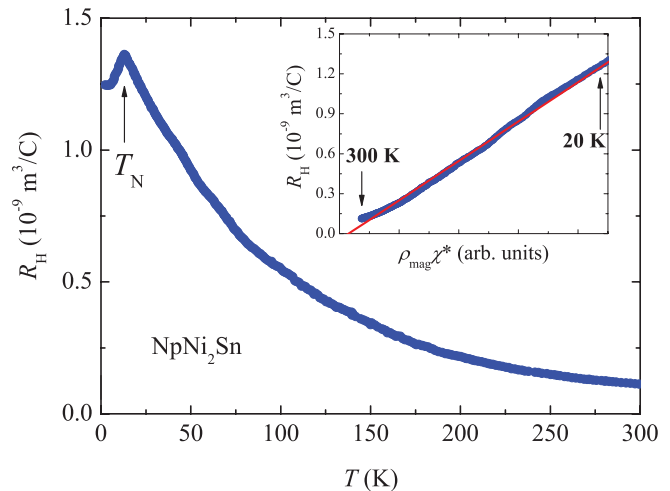


FIG. 4. (Color online) Temperature dependence of the Hall coefficient of NpNi<sub>2</sub>Sn, measured in a field of 14 T. The inset presents the  $R_H$  vs  $\rho_{\text{mag}}\chi^*$  dependence. The solid line denotes the fit of Eq. (4) to the experimental data.

to the electrical resistivity. In the case of NpNi<sub>2</sub>Sn,  $\rho_{\text{mag}}$  can be approximated by the total measured resistivity  $\rho$  (cf. Sec. III C). The inset of Fig. 4 shows  $R_H$  plotted as a function of  $\chi^*\rho_{\text{mag}}$ . From the least-squares fitting of Eq. (4) to these data, one derives  $R_0 = -6.4 \times 10^{-10} \text{ m}^3/\text{C}$  and the coefficient  $\gamma_1 = 0.26 \text{ K/T}$ . The so-obtained  $\gamma_1$  value is nearly one order of magnitude larger than those reported for the Ce-based heavy-fermion systems CeCu<sub>6</sub> and CeAl<sub>3</sub> (Ref. 25) and two orders of magnitude larger than that found for the related system PuPd<sub>2</sub>Sn.<sup>17</sup> The negative value of the ordinary Hall coefficient implies that predominantly electrons carry the electrical current. A simple one-band model provides an estimation of the concentration of free carriers to be  $n = \frac{1}{R_H e} = 0.98 \times 10^{22} \text{ cm}^{-3}$  ( $2.7 \frac{\text{carrier}}{\text{unit cell}}$ ), which is close to the carrier density in heavy-fermion intermetallics, such as CeAl<sub>3</sub> (Ref. 25) and CeNiGe<sub>3</sub>.<sup>26</sup>

#### E. Thermoelectric power

Figure 5 presents the temperature dependence of the Seebeck coefficient of NpNi<sub>2</sub>Sn. At room temperature, the thermopower has a value of about  $3.5 \mu\text{V}/\text{K}$ . It decreases with decreasing temperature, changes sign to negative at about 120 K, and shows a shallow local minimum at 38 K and then a sharp minimum at 10 K, below which it turns toward zero as expected at  $T = 0 \text{ K}$ . At the Néel temperature, the  $S(T)$  curve shows an inflection point (see the inset of Fig. 5). In the framework of the so-called two-band model,<sup>27,28</sup> the temperature variation of the Seebeck coefficient is governed mainly by the scattering of conduction electrons from broad  $s$ - $d$  bands into a narrow  $5f$  quasiparticle band. Assuming that the latter band has a Lorentzian shape of the width  $W$  and it is located at the energy  $\varepsilon_F$  in relation to the Fermi level, the density of states is given by

$$N(E) = \frac{W}{(E - \varepsilon_F)^2 + W^2}. \quad (5)$$

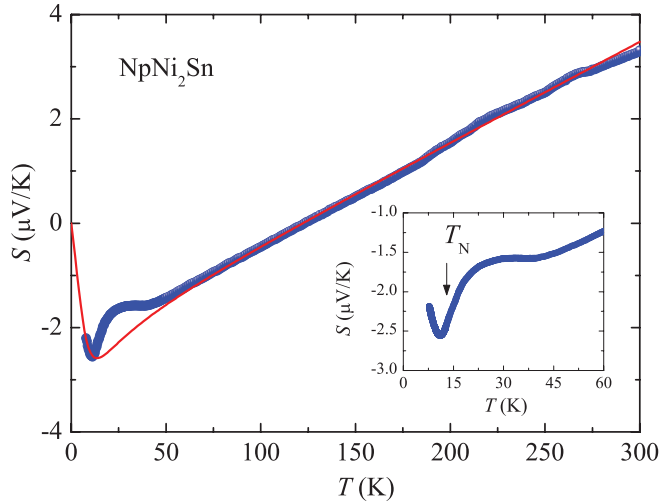


FIG. 5. (Color online) Temperature dependence of the thermoelectric power of  $\text{NpNi}_2\text{Sn}$ . The solid line is the fit of Eq. (7) to the experimental data. The inset presents the low-temperature data. The arrow marks the magnetic phase transition.

Following Freimuth,<sup>29</sup>  $W$  can be assumed to vary with temperature as

$$W(T) = T_f \exp\left(\frac{-T_f}{T}\right), \quad (6)$$

where the parameter  $T_f$  is related to the quasielastic linewidth of the Kondo peak observed in inelastic neutron scattering experiments.<sup>30</sup> With these approximations one obtains<sup>31</sup>

$$S(T) = C_1 T + \frac{C_2 T \varepsilon_F}{\varepsilon_F^2 + W(T)^2}, \quad (7)$$

where the coefficients  $C_1$  and  $C_2$  are temperature-independent parameters, which account for the strength of the nonmagnetic Mott-type scattering and the magnetic scattering, respectively. The least-squares fitting of the above formula to the experimental data of  $\text{NpNi}_2\text{Sn}$  yielded  $C_1 = 0.12 \mu\text{V K}^{-2}$ ,  $C_2 = -3.4 \mu\text{V K}^{-1}$ ,  $\varepsilon_F = 7.8 \text{ K}$ , and  $T_f = 14.6 \text{ K}$ . These values are similar to those derived within the same approach for several  $4f$ - and  $5f$ -electron intermetallics with strong electronic correlations.<sup>17,32</sup> As can be inferred from Fig. 5, the phenomenological two-band model provides a fairly good description of the thermoelectric power of  $\text{NpNi}_2\text{Sn}$ , except for the region between the two minima of  $S(T)$ . The observed feature might arise due to mechanisms which are entirely neglected in the applied approach, such as the phonon-drag contribution, scattering on crystal-field levels, Kondo coherence, and/or correlations related to the antiferromagnetic ordering that sets in at  $T_N = 13 \text{ K}$ .

#### F. $^{237}\text{Np}$ Mössbauer spectroscopy

Figure 6 shows the  $^{237}\text{Np}$  Mössbauer spectra recorded at different temperatures. At 25 K, the spectrum corresponds to a pure quadrupolar interaction ( $|e^2qQ| = 30.2 \text{ mm/s}$ ) as expected in the paramagnetic state. The isomer shift ( $\delta_{\text{IS}} = -5.4 \text{ mm/s}$  vs  $\text{NpAl}_2$ ) suggests that the neptunium ions are in the trivalent state (electronic configuration  $5f^4$ ). At 4.2 K, the spectrum exhibits magnetic splitting due to the

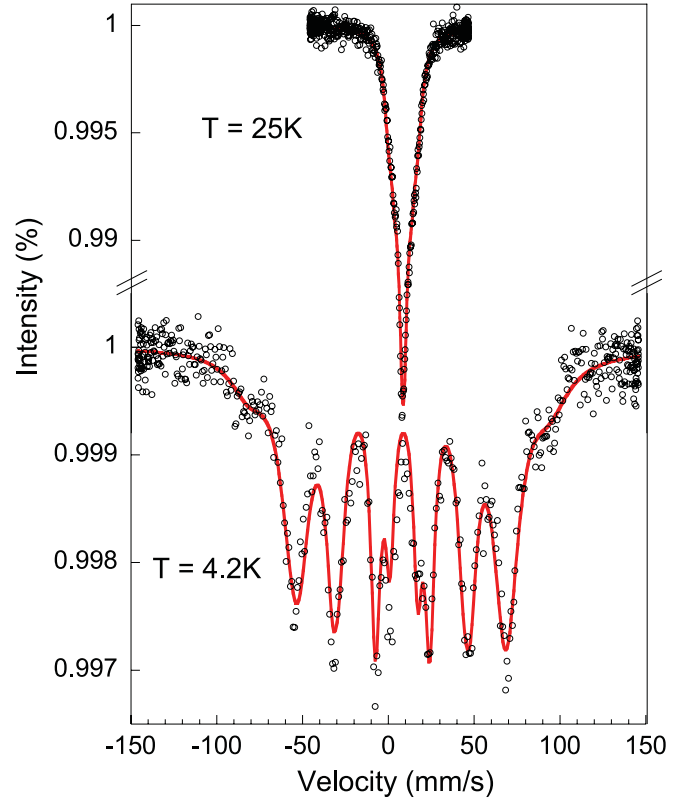


FIG. 6. (Color online)  $^{237}\text{Np}$  Mössbauer spectra of  $\text{NpNi}_2\text{Sn}$  recorded at 25 K and 4.2 K.

degeneracy lift of nuclear levels ( $I = 5/2$ ) by the electronic hyperfine field. The pattern cannot, however, be reproduced by a single static site, and relative intensities point toward relaxation effects. Indeed, the spectrum can be accounted for by the Wegener model,<sup>33</sup> which assumes longitudinal fluctuations of the hyperfine magnetic field around a time-averaged value, found to amount to  $\langle B_{\text{hf}} \rangle = 325 \text{ T}$ . The ordered magnetic moment carried by neptunium is inferred to be  $\mu_{\text{Np}} = 1.51 \mu_B$  and its direction tilted at  $49^\circ$  or  $61^\circ$  (depending on the sign of the quadrupolar interaction parameter in the paramagnetic state, which is not known) from the main component of the electric field gradient.

#### IV. SUMMARY

The Np-based intermetallic compound  $\text{NpNi}_2\text{Sn}$  has been synthesized in polycrystalline form and studied over wide temperature and magnetic-field ranges. It crystallizes with the orthorhombic  $Pnma$  unit cell like the  $An\text{Pd}_2\text{Sn}$  phases. The magnetic susceptibility, the heat capacity, and the electrical resistivity data conjointly signal the antiferromagnetic ordering that sets in at 13 K. The negative Curie temperature with the large absolute value, the negative logarithmic dependence of the electrical resistivity in the paramagnetic region, and the enhanced linear contribution to the heat capacity are all indicative of  $\text{NpNi}_2\text{Sn}$ , belonging to the family of dense Kondo systems. Also, the temperature dependencies of the Hall and Seebeck coefficients are typical for strongly correlated electronic systems. In conclusion,  $\text{NpNi}_2\text{Sn}$  is a novel

antiferromagnetic Kondo lattice, one of very few known amidst Np-based intermetallics.

#### ACKNOWLEDGMENTS

The high-purity Np metal required for the synthesis of NpNi<sub>2</sub>Sn was made available in the framework of the collaboration with the Lawrence Livermore and Los Alamos

National Laboratories and the US Department of Energy. This work was made possible thanks to the support of the European Community Transnational Access to Research Infrastructures Action of the “Strengthening the European Research Area” specific program, Contract No. RITA-CT-2006-026176, in financing the Access to the Actinide User Laboratory at the ITU-Karlsruhe.

- 
- <sup>1</sup>G. R. Stewart, *Rev. Mod. Phys.* **56**, 755 (1984).  
<sup>2</sup>G. R. Stewart, *Rev. Mod. Phys.* **73**, 797 (2001).  
<sup>3</sup>C. Pfleiderer, *Rev. Mod. Phys.* **81**, 1551 (2009).  
<sup>4</sup>J. L. Sarrao, L. A. Morales, J. D. Thompson, B. L. Scott, G. R. Stewart, F. Wastin, J. Rebizant, P. Boulet, E. Colineau, and G. H. Lander, *Nature (London)* **420**, 297 (2002).  
<sup>5</sup>F. Wastin, P. Boulet, J. Rebizant, E. Colineau, and G. H. Lander, *J. Phys.: Condens. Matter* **15**, S2279 (2003).  
<sup>6</sup>D. Aoki, Y. Haga, T. D. Matsuda, N. Tateiwa, S. Ikeda, Y. Homma, H. Sakai, Y. Shiokawa, E. Yamamoto, A. Nakamura *et al.*, *J. Phys. Soc. Jpn.* **76**, 063701 (2007).  
<sup>7</sup>C. Rossel, M. S. Torikachvili, J. W. Chen, and M. B. Maple, *Solid State Commun.* **60**, 563 (1986).  
<sup>8</sup>Z. Żolnierak, *J. Magn. Magn. Mater.* **76–77**, 231 (1988).  
<sup>9</sup>M. Marezio, D. Cox, C. Rossel, and M. Maple, *Solid State Commun.* **67**, 831 (1988).  
<sup>10</sup>T. Takabatake, H. Kawanaka, H. Fujii, Y. Yamaguchi, J. Sakurai, Y. Aoki, and T. Fujita, *J. Phys. Soc. Jpn.* **58**, 1918 (1989).  
<sup>11</sup>T. Takabatake, Y. Maeda, H. Fujii, S. Ikeda, S. Nishigori, T. Fujita, A. Minami, I. Oguro, K. Sugiyama, K. Oda *et al.*, *Phys. B (Amsterdam, Neth.)* **186–188**, 734 (1993).  
<sup>12</sup>C. L. Seaman, N. R. Dilley, M. C. de Andrade, J. Herrmann, M. B. Maple, and Z. Fisk, *Phys. Rev. B* **53**, 2651 (1996).  
<sup>13</sup>I. Maksimov, F. J. Litterst, S. Süllow, and J. A. Mydosh, *Phys. B (Amsterdam, Neth.)* **312–313**, 283 (2002).  
<sup>14</sup>I. Maksimov, F. J. Litterst, H. Rechenberg, M. A. C. de Melo, R. Feyerherm, R. W. A. Hendriks, T. J. Gortenmulder, J. A. Mydosh, and S. Süllow, *Phys. Rev. B* **67**, 104405 (2003).  
<sup>15</sup>K. Gofryk, D. Kaczorowski, and A. Czopnik, *Solid State Commun.* **133**, 625 (2005).  
<sup>16</sup>D. Kaczorowski, K. Gofryk, P. Boulet, J. Rebizant, P. Javorský, E. Colineau, F. Wastin, and G. H. Lander, *Phys. B (Amsterdam, Neth.)* **359–361**, 1102 (2005).  
<sup>17</sup>K. Gofryk, D. Kaczorowski, J.-C. Griveau, N. Magnani, R. Jardin, E. Colineau, J. Rebizant, F. Wastin, and R. Caciuffo, *Phys. Rev. B* **77**, 014431 (2008).  
<sup>18</sup>A. Drost, W. G. Haije, E. Frikkee, T. Endstra, G. J. Nieuwenhuys, and K. H. J. Buschow, *Solid State Commun.* **88**, 327 (1993).  
<sup>19</sup>F. M. Mulder, A. Drost, R. C. Thiel, and E. Frikkee, *Phys. Rev. Lett.* **77**, 3477 (1996).  
<sup>20</sup>T. Endstra, S. A. M. Mentink, G. J. Nieuwenhuys, J. A. Mydosh, and K. H. J. Buschow, *J. Phys.: Condens. Matter* **2**, 2447 (1990).  
<sup>21</sup>M. E. Fisher, *Philos. Mag.* **7**, 1731 (1962).  
<sup>22</sup>S. N. de Medeiros, M. A. Continentino, M. T. D. Orlando, M. B. Fontes, E. M. Baggio-Saitovitch, A. Rosch, and A. Eichler, *Phys. B (Amsterdam, Neth.)* **281–282**, 340 (2000).  
<sup>23</sup>M. A. Continentino, S. N. de Medeiros, M. T. D. Orlando, M. B. Fontes, and E. M. Baggio-Saitovitch, *Phys. Rev. B* **64**, 012404 (2001).  
<sup>24</sup>Y. Suezaki and H. Mori, *Phys. Lett. A* **28**, 70 (1968).  
<sup>25</sup>A. Fert and P. M. Levy, *Phys. Rev. B* **36**, 1907 (1987).  
<sup>26</sup>A. P. Pikul, D. Kaczorowski, T. Plackowski, A. Czopnik, H. Michor, E. Bauer, G. Hilscher, P. Rogl, and Y. Grin, *Phys. Rev. B* **67**, 224417 (2003).  
<sup>27</sup>U. Gottwick, K. Gloos, S. Horn, F. Steglich, and N. Grewe, *J. Magn. Magn. Mater.* **47–48**, 536 (1985).  
<sup>28</sup>M. D. Koterlyn, O. I. Babych, and G. M. Koterlyn, *J. Alloys Compd.* **325**, 6 (2001).  
<sup>29</sup>A. Freimuth, *J. Magn. Magn. Mater.* **68**, 28 (1987).  
<sup>30</sup>E. Holland-Moritz, D. Wohlleben, and M. Loewenhaupt, *Phys. Rev. B* **25**, 7482 (1982).  
<sup>31</sup>C. S. Garde and J. Ray, *Phys. Rev. B* **51**, 2960 (1995).  
<sup>32</sup>D. Kaczorowski and K. Gofryk, *Solid State Commun.* **138**, 337 (2006).  
<sup>33</sup>H. Wegener, *Z. Phys. A* **186**, 498 (1965).